Acta Crystallographica Section B
Structural Science
ISSN 0108-7681

Dipyrimidine–copper(II) dinitrate complexes showing magnetic interactions

Masanori Yasui, Yoshimitsu Ishikawa, Naoya Akiyama, Takayuki Ishida, Takashi Nogami and Fujiko Iwasaki*

Department of Applied Physics and Chemistry, The University of Electro-Communications, Chofu, Tokyo 182-8585, Japan

Correspondence e-mail: fuji@pc.uec.ac.jp

Received 14 September 2000
Accepted 8 February 2001

Crystals of $Cu^{II}(NO_3)_2(pm)_3$ (1), and two crystalline forms of $Cu^{II}(NO_3)_2(H_2O)_2(pm)_2$, (2) and (3), showed ferromagnetic, antiferromagnetic and paramagnetic interactions at extremely low temperatures, respectively. Crystal structure analyses revealed that the complexes were *catena*-dinitrato[μ-pyrimidine-κN^1:κN^3]-(pyrimidine-N^1)copper(II), $[Cu(NO_3)_2(pm)_2]_n$, *catena*-diaquadinitrato[μ-pyrimidine-κN^1:κN^3]copper(II), $[Cu(NO_3)_2(H_2O)_2(pm)]_n$, and diaquadinitratodipyrimidine-copper(II), $Cu(NO_3)_2(H_2O)_2(pm)_2$ for (1), (2) and (3), respectively. In (1) the Cu atom is coordinated by the two nitrates and N atoms of the non-bridging pyrimidine and bridging pyrimidine to form a one-dimensional coordination polymer. The complex is a five-coordinated square pyramid and can be regarded as a pseudo-seven-coordinated complex, since other short non-bonding Cu···O contacts are observed. In the crystals of (2) the pyrimidine bridges the Cu atoms to form a one-dimensional coordination chain. On the other hand, complex (3) is not a coordination polymer. It is important to form a coordination polymer for the appearance of the magnetic interactions. Types of coordination of the bridging organic moieties should also play an important role in magnetic properties. Magnetic measurements of (1) and (2) show that they are good examples of uniform $S = 1/2$ ferro- and antiferromagnetic Heisenberg chains with exchange parameters $2J/kB = +1.8$ and -36 K, respectively.

1. Introduction

Recently many organic coordination compounds containing transition metals as spin sources have been studied to develop magnetic interactions in organic compounds. Some copper(II) transition complexes coordinated with pyrimidines or related compounds which have *meta*-coordination positions showed magnetic interactions (Ishida *et al.*, 1995, 1996, 1997). Among them, complexes of $Cu^{II}(hfac)_2$ (hfac = 1,1,1,5,5,5-hexafluoropentane-2,4-dionate) coordinated by quinazoline, pyrimidine and 4-methylpyrimidine showed ferromagnetic interactions at extremely low temperatures. Structural studies revealed that these complexes formed one-dimensional coordination chains and the interactions between chains were van der Waals type (Ishida *et al.*, 1996; Yasui *et al.*, 2001). In order to improve the molecular interactions, $Cu^{II}(NO_3)_2$ complexes coordinated by pyrimidine (hereafter abbreviated by pm) were synthesized and their magnetic properties were measured (Ishida *et al.*, 1997). The complex $Cu(NO_3)_2(pm)_3$ (1) showed a ferromagnetic interaction. X-ray analysis revealed that the complex $Cu(NO_3)_2(H_2O)_2(pm)_2$ crystallized into two modifications, (2) and (3); the magnetic properties

measured on these crystals separately showed an antiferromagnetic interaction for (2) and a paramagnetic interaction for (3). Crystal structure analyses were performed on these $Cu^{II}(NO_3)_2$ complexes (1)–(3) in order to examine the relations between magnetic interactions and crystal structures.

2. Experimental

Complex (1) was synthesized from copper(II) nitrate trihydrate and pyrimidine, and crystallized from methanol solutions. Crystals of (1) were coated with epoxy resin soon after being produced from the solution, because they were very unstable in air. Crystals of (2) and (3) were obtained from copper(II) nitrate and pyrimidine in water. Two types of crystals were obtained from the same batch. The X-ray analysis revealed that crystals of $Cu(NO_3)_2(H_2O)_2(pm)_2$ showed two modifications, (2) and (3). The intensity data were measured using a Rigaku diffractometer AFC-7*R* with a graphite monochromator. The structures were solved by direct methods using the programs *SIR*88 (Burla *et al.*, 1989) and *DIRDIF*92 (Buerskens *et al.*, 1992). The H atoms were obtained from difference Fourier maps. The structures were refined by full-matrix least-squares with anisotropic temperature factors for non-H atoms and isotropic ones for H atoms.

For (1) intensity measurement was also carried out at 100 K with an N_2-extraction gas-flow device using a different crystal (1*b*) in order to analyze electron densities. For (1*b*), after the refinements with full-matrix least-squares using the program *SHELXL*97 (Sheldrick, 1997) [$R = 0.0366$ for 4958 reflections, $I > 2\sigma(I)$, $wR_2 = 0.1012$ for 7876 reflections with 197 parameters, flack parameter = 0.0350 (9), H atoms were treated as a riding model] and high-order refinements with $\sin\theta/\lambda > 0.6$, further refinements were carried out using the multipole expansion atomic scattering factors by the program *MOLLY*5 (Hansen & Coppens, 1978). Crystal data, details concerning data collection and structure refinements are listed in Table 1.[1]

3. Results and discussions

3.1. Structure of (1)

The molecular structure of (1) along with the atomic numbering and the crystal structure are shown in Figs. 1 and 2, respectively. Selected bond distances and angles are listed in Table 2. The Cu atom is coordinated by O1, O4, N3 and N5 equatorially, and N6^{i} [(i) $x-\frac{1}{2}, 1-y, z$] axially to form a five-coordinated square-pyramidal complex. The Cu atom is coordinated by two types of pyrimidines; one bridges Cu···Cu at the *meta* N atoms to form a one-dimensional chain along the *a* axis, while the other coordinates only at one N atom. In the pyrimidine-bridging chain, —Cu—N—C—N—Cu—N—C—N—, one N atom coordinates axially and the other coordinates equatorially. The axial Cu1—N6^{i} [2.303 (3) Å] is significantly longer than the equatorial Cu1—N3 and Cu1—N5 lengths [2.041 (3) and 2.036 (3) Å, respectively]. In the distorted octahedral complex, $Cu^{II}(hfac)_2(pm)_2$, pyrimidine moieties also bridge the Cu atoms from the axial and equatorial positions with Cu—N_{ax} 2.370 (7) Å and Cu—N_{eq} 2.104 (7) Å. Four other Cu complexes coordinated by pyrimidines were found from the Cambridge Structural Database (CSD; Allen *et al.*, 1991). Two of them are five-coordinated square pyramids with axially and equatorially bridging pyrimidines (Refcodes: LAYNAE; Chen, Fu *et al.*, 1994; ZATGOQ; Chen, Qiu *et al.*, 1994). In these complexes Cu—N_{ax} are 2.35–2.45 Å and

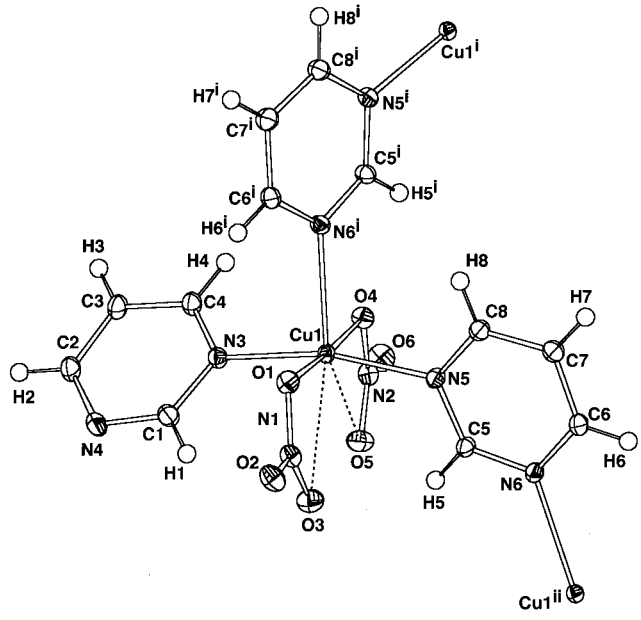

Figure 1
*ORTEP*II (Johnson, 1976) drawing of (1*b*) (100 K) with the atom-numbering. The displacement ellipsoids for non-H atoms are drawn at 50% probability and the H atoms are drawn as spheres with a radius of 0.1 Å. Symmetry codes: (i) $x-\frac{1}{2}, 1-y, z$; (ii) $x+\frac{1}{2}, 1-y, z$.

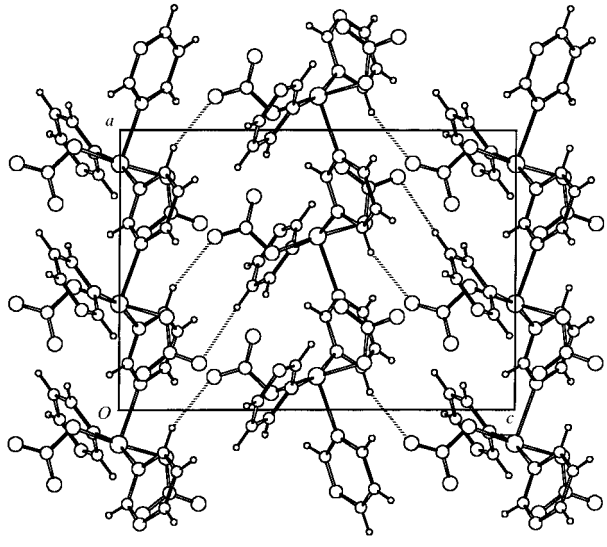

Figure 2
Crystal structure of (1*b*) viewed along the *b* axis. C—H···O contacts are shown with broken lines.

[1] Supplementary data for this paper are available from the IUCr electronic archives (Reference: OA0034). Services for accessing these data are described at the back of the journal.

Table 1
Experimental details.

	(1*a*)	(1*b*)	(2)	(3)
Crystal data				
Chemical formula	$Cu(NO_3)_2(C_4H_4N_2)_2$	$Cu(NO_3)_2(C_4H_4N_2)_2$	$Cu(C_4H_4N_2)(H_2O)_2$-$(NO_3)_2$	$Cu(C_4H_4N_2)_2(H_2O)_2$-$(NO_3)_2$
Chemical formula weight	347.74	347.74	303.68	383.78
Cell setting, space group	Orthorhombic, $Pca2_1$	Orthorhombic, $Pca2_1$	Monoclinic, C_2/c	Monoclinic, $P2_1/a$
a, b, c (Å)	9.991 (5), 8.531 (6), 14.359 (5)	10.000 (2), 8.4519 (2), 14.187 (2)	12.408 (8), 11.511 (9), 7.518 (9)	7.1658 (12), 14.105 (2), 7.5358 (14)
β (°)	90	90	114.99 (5)	114.324 (12)
V (Å^3)	1223.9 (11)	1199.1 (4)	973.2 (15)	694.1 (2)
Z	4	4	4	2
D_x (Mg m^{-3})	1.887	1.926	2.072	1.836
Radiation type	Mo $K\alpha$	Mo $K\alpha$	Mo $K\alpha$	Mo $K\alpha$
No. of reflections for cell parameters	25	25	25	25
θ range (°)	14.8–17.5	14.0–15.6	12.6–16.7	17.2–17.5
μ (mm^{-1})	1.827	1.865	2.289	1.630
Temperature (K)	295	100	294	296
Crystal form, color	Prism, blue	Prism, blue	Prismatic, light blue	Prism, blue
Crystal size (mm)	0.40 × 0.30 × 0.20	0.15 × 0.14 × 0.10	0.40 × 0.40 × 0.30	0.30 × 0.20 × 0.20
Data collection				
Diffractometer	Rigaku AFC-7*R*	Rigaku AFC-7*R*	Rigaku AFC-7*R*	Rigaku AFC-7*R*
Data collection method	ω–2θ scans	ω–2θ scans	ω–2θ scans	ω–2θ scans
Absorption correction	Psi-scan (North *et al.*, 1968)	Analytical (De Meulenaer & Tompa, 1965)	Psi-scan	Psi-scan
T_{min}	0.582	0.749	0.323	0.612
T_{max}	0.711	0.801	0.544	0.734
No. of measured, independent and observed parameters	1464, 1464, 1394	15 315, 7876, 5759	1162, 1113, 1076	1625, 1508, 1291
Criterion for observed reflections	$I > 2\sigma(I)$	$I > 3\sigma(F)$	$I > 2\sigma(I)$	$I > 2\sigma(I)$
R_{int}	0.0000	0.0685	0.0596	0.0427
θ_{max} (°)	27.50	60.0	27.50	26.94
Range of h, k, l	$0 \rightarrow h \rightarrow 12$ $0 \rightarrow k \rightarrow 11$ $-18 \rightarrow l \rightarrow 0$	$-24 \rightarrow h \rightarrow 24$ $-20 \rightarrow k \rightarrow 0$ $0 \rightarrow l \rightarrow 34$	$0 \rightarrow h \rightarrow 16$ $0 \rightarrow k \rightarrow 14$ $-9 \rightarrow l \rightarrow 8$	$0 \rightarrow h \rightarrow 9$ $0 \rightarrow k \rightarrow 17$ $-9 \rightarrow l \rightarrow 8$
No. and frequency of standard reflections	3 every 150 reflections	3 every 100 reflections	3 every 150 reflections	3 every 150 reflections
Intensity decay (%)	0.18	0.997	6.68	2.95
Refinement				
Refinement on	F^2	F	F^2	F^2
$R[F^2>2\sigma(F^2)]$, $wR(F^2)$, S	0.0286, 0.0782, 1.038	0.0384, 0.0339, 1.236	0.0285, 0.0821, 1.152	0.0517, 0.148, 1.079
No. of reflections and parameters used in refinement	1464, 199	5759, 535	1113, 97	1508, 130
H-atom treatment	Riding	Not refined	Refined	Refined
Weighting scheme	$w = 1/[\sigma^2(F_o^2) + (0.0619P)^2 + 0.1183P]$, where $P = (F_o^2 + 2F_c^2)/3$	$w = 1/[\sigma^2(F_o^2)]$	$w = 1/[\sigma^2(F_o^2) + (0.0538P)^2 + 0.8570P]$, where $P = (F_o^2 + 2F_c^2)/3$	$w = 1/[\sigma^2(F_o^2) + (0.1118P)^2 + 0.2222P]$, where $P = (F_o^2 + 2F_c^2)/3$
$(\Delta/\sigma)_{max}$	0.000	0.001	0.001	0.001
$\Delta\rho_{max}$, $\Delta\rho_{min}$ (e Å^{-3})	0.702, −0.598	1.34, −1.44	0.612, −0.866	1.54, −1.321
Extinction method	*SHELXL*97 (Sheldrick, 1997)	None	*SHELXL*97 (Sheldrick, 1997)	None
Extinction coefficient	0.0030 (12)	–	0.104 (4)	–

Computer programs used: *AFC Control Software* (Rigaku Corporation, 1994), *TEXSAN* (Molecular Science Corporation, 1992), *SIR*88 (Burla *et al.*, 1989), *SHELXL*97 (Sheldrick, 1997), *MOLLY*5 (Hansen & Coppens, 1978), *DIRDIF*92 (Beurskens *et al.*, 1992).

Cu—N_{eq} are 2.00–2.01 Å. However, these complexes showed strong antiferromagnetic interactions owing to the *trans*-oxamidato-bridged Cu dimers. The other complexes include one which has a three-dimensional network with tetrahedrally bridging pyrimidines (RIDKOE; Keller, 1997) and another which is an octahedral complex with four equatorial non-bridging pyrimidines (RIQNAG; Novak & Keller, 1997). The bond lengths of Cu—N for these complexes are 2.03–2.15 Å.

The planarity of the equatorial coordination is distorted, as shown from the angles of O1—Cu1—O4, N3—Cu1—N5, N3—Cu1—N6^{i} and N5—Cu1—N6^{i}, which are 175.56 (12), 165.81 (11), 94.09 (12) and 100.05 (11)°, respectively. The dihedral angles between the equatorial O1—O4—N3—N5 plane and the nitrate and pyrimidine planes are 81.24 (12), 89.08 (13), 40.81 (15), 81.96 (10) and 87.36 (10)° for O1—N1—O2—O3, O4—N2—O5—O6, N3—C1—N4—C2—C3—C4,

Table 2
Selected bond lengths and angles (Å, °).

	(1*a*) (295 K)	(1*b*) (100 K)
Cu1—O1	1.990 (3)	2.001 (2)
Cu1—O4	1.978 (3)	1.978 (2)
Cu1—N3	2.041 (3)	2.0268 (19)
Cu1—N5	2.036 (3)	2.0329 (18)
Cu1—N6^{i}	2.303 (3)	2.2928 (18)
O1—N1	1.296 (4)	1.298 (3)
O2—N1	1.232 (4)	1.225 (3)
O3—N1	1.226 (5)	1.245 (3)
O4—N2	1.298 (4)	1.302 (3)
O5—N2	1.230 (4)	1.233 (3)
O6—N2	1.229 (5)	1.229 (3)
Cu1—O3	2.776 (3)	2.799 (2)
Cu1—O5	2.751 (4)	2.742 (2)
O1—Cu1—O4	175.58 (11)	175.95 (9)
O1—Cu1—N3	91.10 (12)	90.81 (9)
O1—Cu1—N5	90.06 (12)	89.68 (8)
O1—Cu1—N6^{i}	90.06 (12)	90.17 (8)
O4—Cu1—N3	88.79 (12)	88.85 (8)
O4—Cu1—N5	91.12 (11)	91.66 (8)
O4—Cu1—N6^{i}	85.54 (11)	85.83 (8)
N3—Cu1—N5	165.84 (11)	165.58 (8)
N3—Cu1—N6^{i}	94.09 (12)	94.04 (7)
N5—Cu1—N6^{i}	100.05 (11)	100.37 (7)
Cu1—O1—N1	113.5 (2)	113.92 (17)
Cu1—O4—N2	112.8 (2)	112.01 (15)
O1—N1—O2	117.7 (3)	118.2 (2)
O1—N1—O3	118.3 (3)	118.2 (2)
O2—N1—O3	124.0 (3)	123.6 (2)
O4—N2—O5	118.0 (3)	118.4 (2)
O4—N2—O6	118.2 (3)	117.9 (2)
O5—N2—O6	123.8 (4)	123.7 (3)
Cu1—N3—C1	121.3 (3)	121.71 (16)
Cu1—N3—C4	121.7 (2)	121.47 (15)
Cu1—N5—C5	119.3 (2)	118.64 (14)
Cu1—N5—C8	123.7 (2)	123.92 (15)
C5—N6—Cu1^{ii}	120.6 (2)	120.00 (14)
C6—N6—Cu1^{ii}	123.0 (2)	122.31 (14)

Symmetry codes: (i) $x-\frac{1}{2}, 1-y, z$; (ii) $x+\frac{1}{2}, 1-y, z$.

N5—C5—N6—C6—C7—C8 and N6^{i}—C5^{i}—N5^{i}—C8^{i}—C7^{i}—C6^{i} planes, respectively.

In the molecule, short non-bonding Cu···O contacts are observed; the lengths of Cu1···O3 and Cu1···O5 are 2.776 (3) and 2.752 (4) Å, respectively. Therefore, (1) can be regarded as a pseudo-seven-coordinated complex. The angles of O—Cu···O are 50.80 (12), 51.43 (10) and 82.60 (11)° for O1—Cu1···O3, O4—Cu1···O5 and O3···Cu1···O5, respectively. The corresponding values at 100 K are 2.799 (2), 2.742 (2) Å, and 50.83 (9), 51.92 (8) and 81.67 (8)°, for Cu1···O3, Cu1···O5, O1—Cu1···O3, O4—Cu1···O5 and O3···Cu1···O5, respectively. Fig. 3 shows the model deformation maps of (1*b*). In Fig. 3(*a*) (the section of the equatorial plane), the lone-paired electrons of O and N atoms coordinated equatorially are clearly shown. The densities of the lone-paired electrons of O3 and O5 are shown in the plane defined by the axial N6^{i}, and equatorial O1 and O4 atoms (Fig. 3*b*). These electron densities point to the Cu atom showing pseudo-coordination. The accuracy of the intensity data, especially at higher θ angles, was inadequate for the detailed discussion of the *d* electrons of the Cu atom. In some Cu complexes with bidentate nitrate groups, found from the CSD, the coordination type is largely a distorted octahedron, where short Cu—O distances of bidentate nitrato groups are 1.959–2.102 Å and long Cu—O distances are 2.541–2.683 Å (COPFOC; Munno & Bruno, 1984; ZEQJIO, Martens *et al.*, 1995).

The lengths of O1—N1 [1.296 (4) Å] and O4—N2 [1.297 (4) Å] in the nitrates are significantly longer than the other N—O bonds [1.225 (5)–1.231 (4) Å], showing the polarizable effect for the strong coordination of Cu1—O1 [1.990 (3) Å] and Cu1—O4 [1.978 (3) Å].

The intrachain Cu1···Cu1^{i} distance is 6.008 (2) Å and the interchain Cu···Cu distances are 7.633 (2) and 8.274 (2) Å for Cu1···Cu1^{iii} [(iii) $\frac{3}{2}-x, y, \frac{1}{2}+z$] and Cu1···Cu1^{iv} [(iv) $1-x, 1-y, \frac{1}{2}+z$], respectively. The corresponding distances at 100 K are 5.9881 (4), 7.5535 (1) and 8.1826 (2) Å for Cu1···Cu1^{i}, Cu1···Cu1^{iii} and Cu1···Cu1^{iv}, respectively. These distances are similar to those of the pyrimidine complexes of Cu^{II}(hfac)$_2$. The contacts between coordination chains are of C—H···O type, of which the dimensions are listed in Table 3.

3.2. Structure of (2)

The molecular structure of (2) along with the atomic numbering is shown in Fig. 4 and the crystal structure is shown

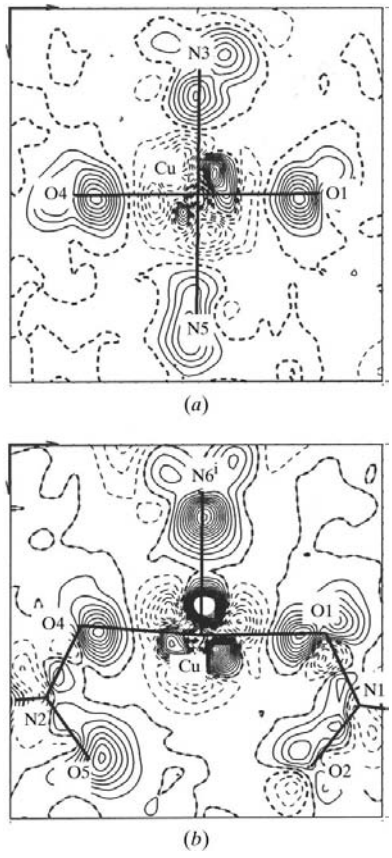

Figure 3
Model-deformation maps, $\Delta\rho$ = ρ[calc,multipole-atom] − ρ[calc, spherical-atom], of (1*b*). (*a*) Section of the equatorial plane; (*b*) section of the O3—Cu1—O5 plane. Solid lines denote positive contours, dashed and dotted lines represent zero and negative contours. Contour intervals: 0.1 e Å^{-3}.

Table 3
Geometry of the intermolecular hydrogen bonds (Å, °).

X—H$\cdots Y$	$X\cdots Y$	H$\cdots Y$	X—H$\cdots Y$
(1*a*)			
C8—H8$\cdots$O6^{iv}	3.310 (5)	2.42	160
C3—H3$\cdots$O2^{v}	3.409 (6)	2.48	178
(1*b*)			
C8—H8$\cdots$O6^{iv}	3.290 (3)	2.38	160
C3—H3$\cdots$O2^{v}	3.372 (3)	2.42	178
(2)			
O4—H41$\cdots$O3^{v}	2.759 (3)	1.93 (3)	176 (2)
O4—H42$\cdots$O3^{vi}	2.782 (4)	2.02 (4)	168 (3)
(3)			
O4—H41$\cdots$O3^{ii}	2.700 (4)	1.87 (5)	168 (4)
O4—H42$\cdots$N3^{iii}	2.769 (4)	1.94 (5)	170 (4)

Symmetry codes: For (1*a*) and (1*b*): (iv) $1-x, 1-y, z+\frac{1}{2}$; (v) $1-x, -y, z-\frac{1}{2}$. For (2): (v) $x, -y, z-\frac{1}{2}$; (vi) $x, y, z-1$. For (3): (ii) $x+1, y, z$; (iii) $x+\frac{1}{2}, \frac{1}{2}-y, z$.

in Fig. 5. Bond distances and angles are listed in Table 4. The Cu1 atom is located at the center of inversion of the crystals and coordinated by two pyrimidines and two water molecules equatorially, and two nitrate anions axially, forming a distorted six-coordinated octahedron. There are no examples of the Cu complexes coordinated with two NO_3 groups and two water molecules in the CSD. The pyrimidine bridges the Cu atoms at the *meta*-N positions to form a one-dimensional coordination chain. The pyrimidine moiety lies in the twofold symmetry of the crystals. In this case, an equatorial–equatorial coordination of pyrimidine is observed along the —Cu—N—C—N—Cu—N—C—N— chain. The length of the axial coordination with NO_3, Cu1—O1 [2.340 (2) Å], is longer than that of Cu—ONO_2 in (1). The lengths of the equatorial coordination with H_2O, Cu1—O4, and pyrimidine, Cu1—N2, are 2.0109 (16) and 2.0315 (18) Å, respectively. A large deviation of the angle of O4—Cu1—O1 [82.22 (8)°] from the right angle shows the

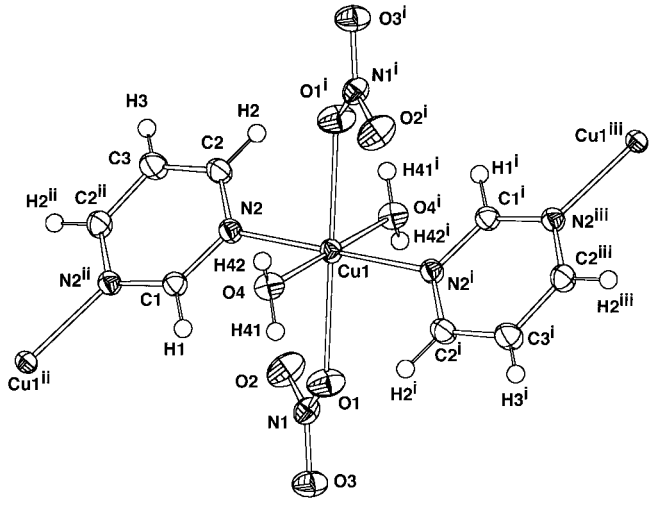

Figure 4
*ORTEP*II (Johnson, 1976) drawing of (2) with the atom numbering. The displacement ellipsoids for non-H atoms are drawn at 50% probability and the H atoms are drawn as spheres with a radius of 0.1 Å. Symmetry codes: (i) $\frac{1}{2}-x, \frac{1}{2}-y, -z$; (ii) $1-x, y, \frac{1}{2}-z$; (iii) $x-\frac{1}{2}, \frac{1}{2}-y, z-\frac{1}{2}$.

Table 4
Selected bond lengths and angles of (2) and (3).

(2)		(3)	
Cu1—O1	2.340 (2)	Cu1—O1	2.435 (3)
Cu1—O4	2.0109 (16)	Cu1—O4	1.973 (2)
Cu1—N2	2.0315 (18)	Cu1—N2	2.017 (2)
O1—N1	1.260 (2)	O1—N1	1.254 (4)
O2—N1	1.224 (2)	O2—N1	1.242 (4)
O3—N1	1.266 (2)	O3—N1	1.240 (4)
O1—Cu1—O4	82.22 (8)	O1—Cu1—O4	91.45 (10)
O1—Cu1—O4^{i}	97.78 (8)	O1—Cu1—O4^{i}	88.55 (10)
O1—Cu1—N2	91.78 (8)	O1—Cu1—N2	93.17 (10)
O1—Cu1—N2^{i}	88.22 (8)	O1—Cu1—N2^{i}	86.83 (10)
O4—Cu1—N2	87.71 (8)	O4—Cu1—N2	89.50 (9)
O4—Cu1—N2^{i}	92.29 (8)	O4—Cu1—N2^{i}	90.50 (9)
Cu1—O1—N1	125.60 (13)	Cu1—O1—N1	123.3 (2)
O1—N1—O2	121.54 (17)	O1—N1—O2	120.1 (3)
O1—N1—O3	117.46 (17)	O1—N1—O3	120.1 (3)
O2—N1—O3	121.00 (18)	O2—N1—O3	119.8 (3)
Cu1—N2—C1	118.55 (14)	Cu1—N2—C1	120.22 (19)
Cu1—N2—C2	123.64 (12)	Cu1—N2—C2	121.9 (2)

Symmetry codes: For (2): (i) $\frac{1}{2}-x, \frac{1}{2}-y, -z$. For (3): (i) $-x, 1-y, -z$.

distortion from the regular octahedron. The dihedral angles between the equatorial O4—N2—O4^{i}—N2^{i} [(i) $\frac{1}{2}-x, \frac{1}{2}-y, -z$] plane and the planes of NO_3, H_2O and the six-membered ring of pyrimidine are 87.44 (10), 80 (3) and 41.62 (8)°, respectively. In the nitrate, the lengths of the O1—N1 [1.260 (2) Å] and the O3—N1 [1.266 (2) Å] bonds are longer than the O2—N1 bond [1.224 (2) Å], but shorter than the N—O bonds related to the strong coordination in (1). The O1 and O3 atoms relate to the coordination and the intermolecular hydrogen bond (see later), respectively, while the O2 atom is free.

The Cu$\cdots$Cu distances are 5.737 (5) and 6.874 (5) Å for the intrachain Cu1$\cdots$Cu1^{ii} [(ii) $1-x, y, \frac{1}{2}-z$] and the interchain Cu1$\cdots$Cu1^{iv} [(iv) $x, 1-y, \frac{1}{2}+z$], respectively. The coordination chains are bound by the hydrogen-bonding network as shown in Fig. 5. Two types of hydrogen bonds are observed between H_2O and NO_3: O4—H41$\cdots$O3^{v} [(v) $x, -y, z-\frac{1}{2}$] and O4—H42$\cdots$O3^{vi} [(vi) $x, y, z-1$]. The geometry of the hydrogen bonds is listed in Table 3.

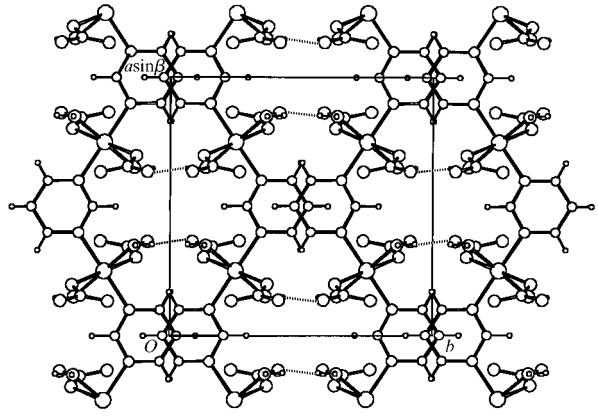

Figure 5
Crystal structure of (2) viewed along the *c* axis. Hydrogen bonds are shown with broken lines.

3.3. Structure of (3)

The molecular structure of (3) along with the atomic numbering is shown in Fig. 6. Bond distances and angles are listed in Table 4. Crystal structure is shown in Fig. 7.

The Cu atom is located at the center of inversion of the crystals and is coordinated by two N atoms of the pyrimidines and two O atoms of the water molecules at the equatorial positions, and two O atoms of the nitrate anions at the axial positions, forming a six-coordinated octahedron. In this instance, unlike (2), the complex is not a coordination polymer. One of the two N atoms of the pyrimidine moiety does not coordinate to the Cu atom. This N atom is used as an acceptor of the intermolecular hydrogen bonding. In the crystals two types of intermolecular hydrogen bond are formed; one is between the water molecule and the nitrate, O4—H41···O3^{ii} [(ii) $x+1, y, z$], and the other is between the water molecule and the pyrimidine, O4—H42···N3^{iii} [(iii) $x+\frac{1}{2}, -y+\frac{1}{2}, z$]. The network of the hydrogen bonds and the dimensions are shown in Fig. 7 and Table 3, respectively. The geometry of the octahedron of (3) is different from that of (2). The axial Cu1—O1 bond [2.435 (3) Å] of (3) is longer than that of (2) [2.340 (2) Å]. The deviations of the bond angles of O1—Cu1—O4 and O1—Cu1—N2 from 90° are less than those of (2), which reflects the weak coordination of Cu1—O1 in (3). The dihedral angles between the equatorial plane and NO_3, H_2O and pyrimidine planes are 35.05 (17), 55 (3) and 52.89 (10)°, respectively. These values are also quite different from those of (2). The deviation of the NO_3 moiety from the regular triangle is the smallest among these three complexes.

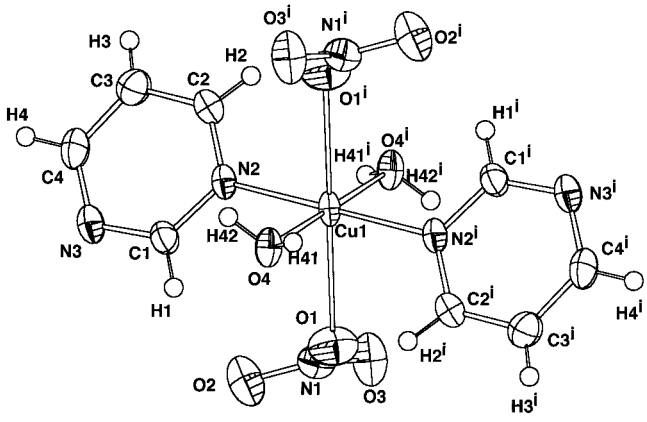

Figure 6
*ORTEP*II (Johnson, 1976) drawing of (3) with the atom numbering. The displacement ellipsoids for non-H atoms are drawn at 50% probability and the H atoms are drawn as spheres with a radius of 0.1 Å. Symmetry code: (i) $-x, 1-y, -z$.

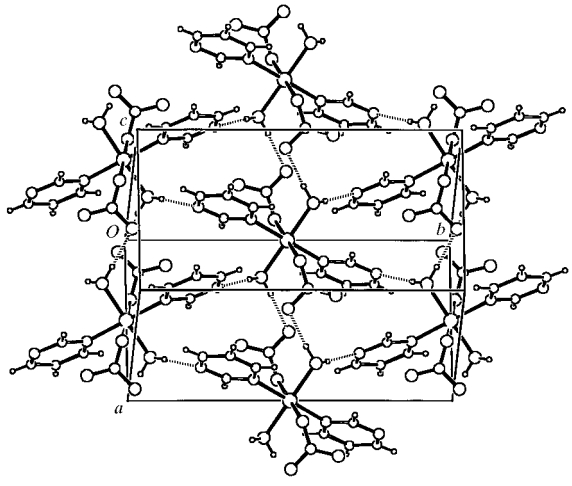

Figure 7
Perspective view of the crystal structure of (3). Hydrogen bonds are shown with broken lines.

3.4. Magnetism

Fig. 8 shows the temperature dependence of $\chi_{mol}T$ (χ_{mol} = molar magnetic susceptibility) for (1), (2) and (3), in which the data were collected on an MPMS-7 SQUID magnetometer (Quantum Design) down to 1.8 K at 0.5 T for the polycrystalline samples (Ishida *et al.*, 1997). The $\chi_{mol}T$ value is proportional to the square of the effective magnetic moment and consequently indicates magnetic interactions in the specimens especially at low temperatures. The $\chi_{mol}T$ value is almost constant for (3), indicating the absence of any appreciable magnetic interaction among the Cu^{II} spins. This paramagnetism agrees well with the isolated mononuclear structure of (3) described above.

A monotonous increase in the $\chi_{mol}T$ of (1) with a decrease in temperature clearly indicates the presence of ferromagnetic interactions. In order to confirm the presence of ferromagnetic interactions the magnetization curve was measured at 1.8 K up to 7 T. The data obtained exceeded the theoretical Brillouin function of $S = 1/2$ and fell between those of $S = 1$ and 3/2. The exchange parameter J (defined by a spin Hamiltonian $H = -2JS_i \cdot S_{i+1}$) between the neighboring Cu^{II} spins can be

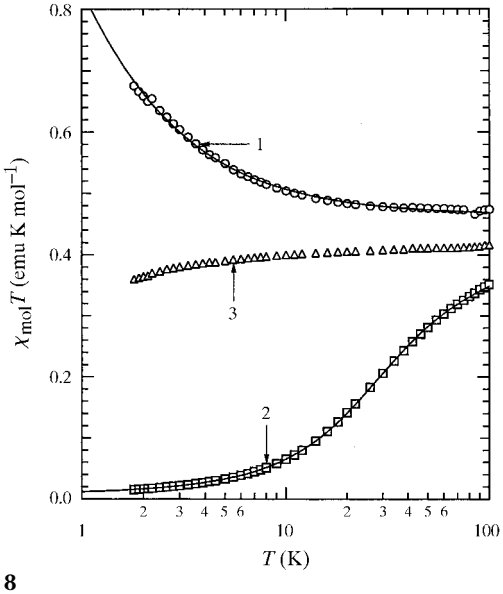

Figure 8
Temperature dependences of the product $\chi_{mol}T$ for (1) (circles), (2) (squares) and (3) (triangles). The solid lines are best-fit curves. See text for the parameters and equations.

estimated from the $\chi_{mol}T$ *versus* T plot. Positive and negative J imply ferro- and antiferromagnetic couplings, respectively. An expression of a high-temperature series (HTS) expansion of magnetic susceptibility as a function of temperature has been proposed for uniform $S = 1/2$ ferromagnetic Heisenberg chains (Baker *et al.*, 1964). A best fit to the above expression gave $2J/k_B = +1.78$ (2) K and $g = 2.23$ (1).

The antiferromagnetic behavior was found for (2), as indicated by a decrease in $\chi_{mol}T$ with a decrease in temperature. The general behavior for uniform $S = 1/2$ antiferromagnetic Heisenberg chains has been analyzed (Bonner & Fisher, 1964). However, fits of the data of (2) to the Bonner–Fisher equation alone gave unsatisfactory results, because of the presence of some additional contribution which is not expected from the ideal chain. The observed temperature dependence of $\chi_{mol}T$ can be well described by the sum of Bonner–Fisher and Curie terms, affording $2J/k_B = -36.8$ (2) K and $g = 2.12$ (1) with a 1.7 (1)% Curie contribution. An HTS expansion is valid for both positive and negative J (Kahn, 1993), and a fit of the data in a temperature range above 23 K (a peaking temperature of χ_{mol}) to this equation gave $2J/k_B = -35.3$ (2) K and $g = 2.13$ (1), assuming that the Curie term is negligible. The $|2J|/k_B = 36$ K of (2) is larger than those of the pyrazine-bridged antiferromagnetic compounds, $Cu(L)(NO_3)_2$ (L = pyrazine derivatives, $2J/k_B = -4$ to -18 K; Richardson & Hatfield, 1976). The molecular orbital calculation analysis suggests that the through-space interaction between two nitrogen lone pairs within a pyrimidine molecule plays an important role in the exchange mechanism for a pyrimidine-bridged dinuclear model compound (Mohri *et al.*, 1999). The large negative value of J of (2) is ascribed to a short N···N distance in pyrimidine compared with those of pyrazines.

Usually, Curie contributions found in antiferromagnetic chain compounds are attributed to impurity spins (such as chain defects). However, a single crystal of (2) showed the strong anisotropy of the Curie contribution by a factor as large as six (Feyerherm *et al.*, 1999). This finding indicates that the Curie contribution is intrinsic for the antiferromagnetic chain. A similar anisotropic Curie contribution has been reported for the one-dimensional antiferromagnetic compound, copper(II) benzoate (Date *et al.*, 1970). Furthermore, a field-induced spin-excitation gap has been extensively investigated in connection with the effective staggered magnetic field in copper(II) benzoate (Dender *et al.*, 1997; Oshikawa & Affleck, 1997). It is well known that the uniform $S = 1/2$ antiferromagnetic chains have a gapless continuum of spin excitations (Bonner & Fisher, 1964). The origin of the Curie contribution as well as a possible spin-excitation gap of the $S = 1/2$ chain in the crystal of (2) can be accounted for by the structural features in the chain: the relative canting g-tensor principal axes of the neighboring copper(II) ions. The Cu—O(nitrate) (Cu1—O1) bond is tilted from the octahedral axis by approximately 8°, as shown from the bond angles. The angle between the Cu1—O1 and the neighboring Cu—O bond along the chain [Cu1^{ii}—O1^{ii}, (ii) $1-x, y, \frac{1}{2}-z$] is 106.90 (11)° and the dihedral angle between the equatorial planes of neighboring Cu^{II} ions [O4—N2—O4^{i}—N2^{i}, (i) $\frac{1}{2}-x, \frac{1}{2}-y, -z$, and O4^{ii}—N2^{ii}—O4^{vii}—N2^{vii}, (vii) $x+\frac{1}{2}, \frac{1}{2}-y, z+\frac{1}{2}$] is 58.80 (8)°.

As shown by the solid lines in Fig. 8, the calculations with the optimized parameters reproduce well the experimental data. Therefore, (1) and (2) can be regarded as almost ideal one-dimensional ferromagnetic and antiferromagnetic chains, respectively. Although the networks of hydrogen bonding are found among the chains for both and seem important to construct the crystal structures, they did not function as magnetic couplers.

3.5. Relations between magnetic interactions and coordination structure

The pyrimidine bridge can work as both ferromagnetic and antiferromagnetic couplers. There are no significant differences in the C—N_{pm}(eq) lengths between complexes exhibiting different magnetic interactions. The dimensions of the pyrimidine moieties show no significant differences between bridging and non-bridging coordinations. The crucial difference is the coordination types of the *meta*-N atoms of the bridging pyrimidine: an axial–equatorial coordination was observed in (1), showing ferromagnetic interactions. Similarly, axial–equatorial coordination types were found in Cu^{II}(hfac)$_2$(qn), Cu^{II}(hfac)$_2$(pm) and Cu^{II}(hfac)$_2$(4-Me-pm), all of which show ferromagnetic interactions. On the other hand, an equatorial–equatorial coordination was observed in (2), showing antiferromagnetic interactions.

The superexchange mechanism is usually discussed concerning the atomic orbital(s) on a closed-shell bridging atom, but in the present study this mechanism should be applied to the molecular orbital on the bridging pyrimidine molecule. The magnetic orbital $d_{x^2-y^2}$ of the copper(II) ion is located on the equatorial plane. The magnetic coupling can be explained in terms of orbital overlaps between a molecular orbital of the pyrimidine and two Cu^{II} $d_{x^2-y^2}$ orbitals. With appreciable overlaps on both sides of the pyrimidine, the magnetic coupling is expected to be antiferromagnetic. When one N atom of pyrimidine is axially coordinated to the copper(II) ion, there is no orbital overlap between the Cu $d_{x^2-y^2}$ and N $n\sigma$ and $p\pi$ orbitals due to orthogonality. Thus, the axial–equatorial combination favors ferromagnetic interactions. A semi-empirical molecular orbital analysis is described elsewhere (Mohri *et al.*, 1999).

This work was supported in part by a Grant-in-Aid for Scientific Research (No. 08454180) and a Grant-in-Aid for Scientific Research on Priority Areas 'Molecular Conductors and Magnets' and 'Metal Assembled Complexes' (Area Nos. 730/11 224 204 and 401/11 136 212, respectively) from the Ministry of Education, Science, Sports and Culture.

References

Allen, F. H., Davies, J. E., Galloy, J. J., Johnson, O., Kennard, O., Macrae, C. F., Mitchell, E. M., Mitchell, G. F., Smith, J. M. & Watson, D. G. (1991). *J. Chem. Inf. Comput. Sci.* **31**, 187–204.

Baker, G. A. Jr, Rushbrooke, G. S. & Gilbert, H. E. (1964). *Phys. Rev. A*, **135**, 1272–1277.
Beurskens, P. T., Admiraal, G., Beurskens, G., Bosma, W. P., Garcia-Granda, S., Gould, R. O., Smits, J. M. M. & Smykalla, C. (1992). *DIRDIF*92. Technical Report, Crystallography Laboratory, University of Nijmegen, The Netherlands.
Bonner, J. C. & Fisher, M. E. (1964). *Phys. Rev. A*, **135**, 640–658.
Burla, M. C., Camalli, M., Cascarano, G., Giacovazzo, C., Polidori, G., Spagna, R. & Viterbo, D. (1989). *J. Appl. Cryst.* **22**, 389–303.
Chen, Z. N., Fu, D. G., Yu, K. B. & Tang, W. X. (1994). *J. Chem. Soc. Dalton Trans.* pp. 1917–1921.
Chen, Z. N., Qiu, J., Tang, W. X. & Yu, K. B. (1994). *Inorg. Chim. Acta*, **224**, 171–176.
Date, M., Yamazaki, H. & Motokawa, M. (1970). *Suppl. Prog. Theor. Phys.* **46**, 194–209.
De Meulenaer, J. & Tompa, H. (1965). *Acta Cryst.* **19**, 1014–1018.
Dender, D. C., Hammar, P. R., Reich, D. H., Broholm, C. & Aeppli, G. (1997). *Phys. Rev. Lett.* **79**, 1750–1753.
Feyerherm, R., Ishida, T., Nogami, T. & Steiner, M. (1999). *Mol. Cryst. Liq. Cryst.* **355**, 235–244.
Hansen, N. K. & Coppens, P. (1978). *Acta Cryst.* A**34**, 909–921.
Ishida, T., Mitsubori, S., Nogami, T., Ishikawa, Y., Yasui, M., Iwasaki, F., Iwamura, H., Takeda, N. & Ishikawa, M. (1995). *Synth. Met.* **71**, 1791–1792.
Ishida, T., Nakayama, K., Nakagawa, M., Sato, W., Yasui, M., Iwasaki, F. & Nogami, T. (1997). *Synth. Met.* **85**, 1655–1658.
Ishida, T., Nogami, T., Yasui, M., Iwasaki, F., Iwamura, H., Takeda, N. & Ishikawa, M. (1996). *Mol. Cryst. Liq. Cryst.* **279**, 87–96.
Johnson, C. K. (1976). *ORTEP*II, Report ORNL-5138. Oak Ridge National Laboratory, Tennessee, USA.
Kahn, O. (1993). *Molecular Magnetism*, ch.11, Section 11.1, pp. 251–257. Weinheim: VCH Publishers.
Keller, S. W. (1997). *Angew. Chem. Engl. Ed.* **36**, 247–248.
Martens, C. F., Schenning, A. P. H. J., Feiters, M. C., Berens, H. W., van der Linden, J. G. M., Admiraal, G., Beurskens, P. T., Kooijman, H., Spek, A. L. & Nolte, R. J. M. (1995). *Inorg. Chem.* **34**, 4735–4744.
Mohri, F., Yoshizawa, K., Yamabe, T., Ishida, T. & Nogami, T. (1999). *Mol. Engng.* **8**, 357–373.
Molecular Science Corporation (1992). *TEXSAN*. MSC, 3200 Research Forest Drive, The Woodlands, TX 77381, USA.
Munno, G. D. & Bruno, G. (1984). *Acta Cryst.* B**40**, 2030–2032.
North, A. C. T., Phillips, D. C. & Mathews, F. S. (1968). *Acta Cryst.* A**24**, 351–359.
Novak, B. & Keller, S. W. (1997). *J. Chem. Cryst.* **27**, 279–282.
Oshikawa, M. & Affleck, I. (1997). *Phys. Rev. Lett.* **79**, 2883–2886.
Richardson, H. W. & Hatfield, W. E. (1976). *J. Am. Chem. Soc.* **98**, 835–839.
Rigaku Corporation (1994). *AFC Control Software.* Rigaku Corporation, Tokyo, Japan.
Sheldrick, G. M. (1997). *SHELXL*97. University of Göttingen, Germany.
Yasui, M., Ishikawa, Y., Ishida, T., Nogami, T. & Iwasaki, F. (2001). To be published.